

Article

Identification of the Functional Modules of SIPP2C.D—SISAUR and Their Roles in Abscisic Acid-Mediated Inhibition of Tomato Hypocotyl Elongation

Xiaolin Zheng^{1,2}, Shihong Fei¹, Shajun Wang¹, Yong He¹ , Zhujun Zhu^{1,*}  and Yuanyuan Liu^{1,*} 

¹ Collaborative Innovation Center for Efficient and Green Production of Agriculture in Mountainous Areas of Zhejiang Province, Key Laboratory of Quality and Safety Control for Subtropical Fruit and Vegetable, Ministry of Agriculture and Rural Affairs, College of Horticulture Science, Zhejiang A&F University, Hangzhou 311300, China

² School of Forestry and Biotechnology, Zhejiang A&F University, Hangzhou 311300, China

* Correspondence: zhuzj@zafu.edu.cn (Z.Z.); yylliu@zafu.edu.cn (Y.L.)

Abstract: The plant hormone ABA regulates various physiological processes, such as promoting stomatal closure and inhibiting hypocotyl elongation by mediating de-phosphorylation of H⁺-ATPase. However, the mechanism acting on ABA-induced de-phosphorylation of H⁺-ATPase remains largely unknown. *SMALL AUXIN UP RNAs (SAURs)*, the largest family of early auxin-response genes, were well-reported to bind to and inhibit PP2C.D phosphatases to maintain plasma membrane H⁺-ATPase activity. In this study, we aimed to investigate whether SAUR-PP2C.D functional modules were involved in ABA-mediated inhibition of hypocotyl elongation. Here, we show that ABA suppresses hypocotyl elongation in both light-grown and dark-grown tomato seedlings in a dose-dependent manner. Hypocotyl elongation of dark-grown seedlings was more sensitive to ABA compared to that of light-grown seedlings. ABA upregulates seven *SIPP2C.D* genes. *SIPP2C.D1* was highly expressed in hypocotyl and upregulated by light. Y2H data showed *SIPP2C.D1* interacted with SISAUR2, 35, 40, 55, 57, 59, 65, and 70. The other four *SIPP2C.Ds* were also associated with a subset of SAUR proteins. Our findings have provided new insights for further examination on the SAUR-PP2C.D modules that regulate outputs of ABA and other phytohormones controlling plant growth and development.

Keywords: *Solanum lycopersicum*; abscisic acid; hypocotyl elongation; SAUR-PP2C.D



Citation: Zheng, X.; Fei, S.; Wang, S.; He, Y.; Zhu, Z.; Liu, Y. Identification of the Functional Modules of SIPP2C.D—SISAUR and Their Roles in Abscisic Acid-Mediated Inhibition of Tomato Hypocotyl Elongation. *Agronomy* **2022**, *12*, 2542. <https://doi.org/10.3390/agronomy12102542>

Academic Editor: Christina Eynck

Received: 2 September 2022

Accepted: 15 October 2022

Published: 18 October 2022

Publisher's Note: MDPI stays neutral with regard to jurisdictional claims in published maps and institutional affiliations.



Copyright: © 2022 by the authors. Licensee MDPI, Basel, Switzerland. This article is an open access article distributed under the terms and conditions of the Creative Commons Attribution (CC BY) license (<https://creativecommons.org/licenses/by/4.0/>).

1. Introduction

Hypocotyl is an important structure connecting the root system to the stem and leaf of higher plants in the embryo and late embryo stages, acting as an important channel for the transport of water, mineral elements, and signaling molecules [1]. Therefore, hypocotyl elongation is an important process for higher plants to adapt to environmental changes, driving seedlings to break through the soil layer for light morphogenesis and photosynthesis. Thus, this process is very sensitive to a variety of signaling molecules (such as hormones) and environmental stimuli (such as light, temperature, and gravity). Light is one of the most important environmental factors affecting plant growth and development, whereas phytohormones such as auxins, abscisic acid (ABA), cytokinins, gibberellins, ethylene, brassinosteroids, salicylic acid, and jasmonic acid may act as second messengers in the regulation of hypocotyl elongation by light [2]. Among them, auxin is essential for hypocotyl elongation. Auxin-induced hypocotyl elongation can be explained by the acid growth theory proposed in the 1970s [3,4]. According to the acid growth theory, auxin activates plasma membrane H⁺-ATPases (PM H⁺-ATPases), which mediate hydrogen ion excretion into the cell wall compartment (apoplast), resulting in apoplastic acidification. The reduced pH in the wall activates cell-wall-loosening enzymes, including expansins [5], xyloglucan endotransglycosylase/hydrolases [6], and pectin methylesterases [7], and initiates the enlargement of the cell. These processes cooperatively facilitate K⁺ ions uptake,

increase water uptake into cells, and trigger cell expansion [8,9]. The mechanism through which auxin might activate PM H⁺-ATPases is reported: auxin promotes phosphorylation of the penultimate threonine residue in the C-terminal auto-inhibitory domain of PM H⁺-ATPases [10], for example, the phosphorylation of Thr-948 and Thr-947 in *Arabidopsis thaliana* plasma membrane proton ATPase1 (AHA1) and AHA2, respectively [11,12]. Phosphorylated Thr-947 allows 14-3-3 protein to bind the C-termini of the ATPases, thus releasing the C-terminal auto-inhibitory structure so as to activate the ATPases [11,13]. Many signals regulate phosphorylation levels of the penultimate threonine in the C-terminus of H⁺-ATPase, including light [14,15], sucrose [16], mannitol [16], bacterial flagellin (flg22) [17], the fungal toxin fusicoccin (FC) [15,18,19], and auxin [10,20], ABA [21], gibberellic acid [20], and cytokinin [20].

It should be noted that, in addition to the penultimate threonine (corresponding to Thr-947 of AHA2), H⁺-ATPase is phosphorylated at multiple sites, including Thr-881, Ser-899, Ser-904, Ser-931, Ser-944, Tyr-946, and Ser-904 [11,17,22–25]. Phosphorylation status exerts a pronounced effect on the activity of the PM H⁺-ATPase. When AHA2 is phosphorylated at Thr-947 or Thr-881, AHA2 is in the upregulated state. However, regardless of whether Thr-947 is phosphorylated, phosphorylation of Ser-931 and Thr-924 inactivate the PM H⁺-ATPase by preventing AHA2 from binding to 14-3-3 proteins. Phosphorylation at Ser-899 also downregulates PM H⁺-ATPase [26].

Protein phosphorylation is coordinated by the protein kinases and protein phosphatases. Previous studies have shown that Ser-931 site of the PM H⁺-ATPase AHA2 is phosphorylated by Ser/Thr protein kinase PKS5 [23]. In addition, the PM-localized leucine-rich repeat receptor kinase (LRR-RLK) plant-peptide-containing sulfated tyrosine 1 receptor (PSY1R) can phosphorylate AHA2/AHA1 at Thr-881 and activate PM H⁺-ATPase activity [27]. FERONIA receptor kinase mediates RALF's inhibitory effect on root elongation by phosphorylating AHA2 at Ser-899 and thus inhibiting the activity of AHA2 [26]. Transmembrane kinase 1 (TMK1) is the protein kinase responsible for auxin-inducible phosphorylation of H⁺-ATPases AHA1 at Thr-948. Auxin promotes the interaction between TMK1 and H⁺-ATPases and thereby activates H⁺-ATPase and promotes cell-wall acidification and hypocotyl cell elongation in Arabidopsis [28]. Recent evidence demonstrates that Ser-944 residue of AHA2 could be phosphorylated by LRR-RLK BRI1-associated receptor kinase 1 (BAK1), which is required for ABA-induced stomatal closure [29].

Phosphorylation and dephosphorylation of PM H⁺-ATPase were reversed by protein kinases and phosphatases. Plant protein phosphatases according to their substrate specificity could be classified into tyrosine phosphatases (PTPs), serine/threonine phosphatases (PSPs), and dual-specificity phosphatases (DSPTPs) [30]. Based on their distinct amino acid sequences and crystal structures, PSPs are further divided into phosphoprotein phosphatases (PPP) and phosphoprotein metallophosphatase (PPM) [31]. The PPP family includes PP1, PP2A, PP2B, PP4, PP5, PP6, and PP7, whereas the PPM family has PP2C and pyruvate dehydrogenase phosphatase [32]. Recent studies indicated that auxin-mediated PM H⁺-ATPase activation and apoplastic acidification not only through TMK1-based cell-surface auxin signaling but also through TIR1/AFB-dependent nuclear auxin perception. Auxin is recognized by TIR1/AFB-Aux/IAA nuclear co-receptor and activates downstream SAUR proteins. Then, SAURs interact and antagonize D-clade PP2C phosphatases (PP2C-Ds), which dephosphorylate Thr-947 phosphorylation of PM H⁺-ATPases [33]. SAURs are the largest family of early auxin-response genes [34]. In addition to auxin, brassinosteroids, gibberellins, jasmonates, and ABA have been reported to regulate the expression of some SAUR genes, indicating that SAURs likely act downstream of various hormones to regulate plant growth and development [34].

ABA has always been regarded as a “stress hormone” that helps plant to adapt to abiotic and biotic stresses. Under control conditions, basal ABA is also essential for growth and development, including seed development, seed dormancy, seed germination, root and hypocotyl elongation, lateral root formation, and chloroplast biogenesis [35,36]. The inhibiting effect of ABA on elongation in etiolated squash hypocotyl segments was

reported about 30 years ago [37]. In 2014, Hayashi et al. [21] found that ABA suppresses hypocotyl elongation in etiolated seedlings through dephosphorylating Thr947 of AHA2 in an ABI1-dependent manner. Recently, ABI1 was demonstrated to directly interact with the C terminus of AHA2 and dephosphorylate Thr947 [38]. ABI1 is one member of clade A protein phosphatases type 2C (PP2Cs) and negatively regulates ABA signaling [39]. Together, PP2Cs were proposed to regulate the phosphorylation and activity of PM AHA activity to mediate the outputs on hypocotyl elongation from auxin and ABA signaling. However, whether ABA-mediated hypocotyl elongation is dependent on PP2Cs-H⁺-ATPase remains unknown.

In the present study, we examined the effect of ABA on the hypocotyl elongation in light-grown and dark-grown seedlings of tomato. Additionally, we characterized the *SIPP2C.D* genes in tomato, then investigated the effect of ABA on expression of these *SIPP2C.D* genes and their tissue-specific expression patterns. Finally, the interactions between *SIPP2C-D* phosphatases and *SISAUR* proteins were demonstrated by the yeast two-hybrid (Y2H) analysis. Overall, this study has shown several SAUR-PP2C.D regulatory modules, which warrants further research on the mechanism of ABA-mediated hypocotyl elongation.

2. Materials and Methods

2.1. Plant Materials and Growth Conditions

Tomato (*Solanum lycopersicum* cv. "Ailsa Craig") was used as the wild type (WT). Tomato seeds were germinated at 25 °C in the dark on filter paper in Petri dishes after sterilization with 15% (*v/v*) NaClO. Consistently germinating seeds were then transferred onto the half-strength Murashige and Skoog medium with 0 (Control), 0.01, or 0.1 μM ABA. Light-grown tomato seedlings were kept in a growth chamber at 25 °C with 16 h light (200 μmol m⁻² s⁻¹) and at 16 °C with 8 h dark. The light source was provided by LED lamps that are specific for plant growth. The lamps emit white light with a full spectrum, including the red and blue spectrum that is necessary for plant growth as well as the far-red spectrum that is supplementary for plant growth. Dark-grown tomato seedlings were wrapped in aluminum foil and kept in the same growth chamber under the same temperature regime.

2.2. Root Length and Shoot Length Measurement

Tomato seedlings were measured on the indicated days. Root lengths were measured from the junction between root and hypocotyl to the root tip, and the hypocotyl length was measured from the junction between root and hypocotyl to the junction between hypocotyl and cotyledon.

2.3. Conserved Domain Analysis

Accession numbers of *SIPP2C.D* genes were derived from a previously published study [40]. Protein sequence of each *SIPP2C.D* gene was downloaded from Sol Genomics Network (<https://solgenomics.net/> (accessed on 26 May 2022)), and conserved domains were annotated via Conserved Domain Search Service (<https://www.ncbi.nlm.nih.gov/Structure/cdd/wrpsb.cgi> (accessed on 26 May 2022)).

2.4. RNA Extraction and Quantitative RT-PCR (qRT-PCR) Analysis

RNA was extracted using TRIzolTM reagent (Invitrogen, Waltham, MA, USA), then one microgram of DNA-free RNA was transcribed into first-strand cDNA by Prime-ScriptTM RT Master Mix (TaKaRa, Kusatsu, Japan). The qRT-PCR was carried out with the UVP ChemStudio (analyticjena) using TB Green Premix Ex Taq (TaKaRa). The reaction conditions were 95 °C for 30 s and 40 cycles at 95 °C for 5 s and 60 °C for 30 s. Expression levels of target genes were normalized relative to the *ACTIN2* gene by the ΔCt method. Primers used to quantify gene expression levels are listed in Table S1. Each reaction was performed with three biological replicates.

2.5. Organ-Specific Expression Analysis

The organ-specific patterns of *SIPP2C.D* genes were analyzed by using RNA-seq data from Tomato Functional Genomics Database (<http://ted.bti.cornell.edu/cgi-bin/TFGD/digital/home.cgi> (accessed on 7 August 2022)). Transcriptome data of eleven tissues of wild species *S. pimpinellifolium* (LA1589) were downloaded. Eleven different tissues include newly developed leaves around 5 mm long, mature green leaflets, flower buds 10 days before anthesis or younger, flowers at anthesis, fruit 10 days post anthesis (10 DPA), fruit 20 days post anthesis (20 DPA), and fruit 33 days post anthesis (33 DPA). RPKM (reads per kilobase million) values are an average of 4 replicates. RPKM values of *SIPP2C.D* genes were log₂-transformed, and heat maps of *SIPP2C.D* genes in different tissues were generated using TBtools v1.098745 software [41].

2.6. Polygenetic Tree by Maximum-Likelihood Method

The polygenetic tree was inferred by using the maximum-likelihood method and JTT matrix-based model. The tree with the highest log likelihood (−13,078.68) is shown. The percentage of trees in which the associated taxa clustered together is shown next to the branches. Initial tree(s) for the heuristic search were obtained automatically by applying neighbor-joining and BioNJ algorithms to a matrix of pairwise distances estimated using the JTT model and then selecting the topology with superior log likelihood value. The tree is drawn to scale, with branch lengths measured in the number of substitutions per site. This analysis involved 23 amino acid sequences. There were a total of 1353 positions in the final dataset. Evolutionary analyses were conducted in MEGA X [42]. Accession numbers of *AtPP2C.D* genes were derived from a previously published study [43]. Protein sequence of each *AtPP2C.D* gene was downloaded from The Arabidopsis Information Resource (<https://www.arabidopsis.org/> (accessed on 26 May 2022)).

2.7. Y2H Assays

The Y2H assays were performed using the Matchmaker GAL4 Two-Hybrid System (Clontech). Full-length CDSs of *SISAUR* genes were cloned into the *pGADT7* vector, and full-length CDSs of *SIPP2C.D* genes were cloned into the *pGBKT7* vector. Primers used for plasmid construction are listed in Table S1. Constructs used to test protein–protein interactions were co-transformed into yeast (*Saccharomyces cerevisiae*) strain AH109. Co-transformation of empty *pGADT7* vectors served as a negative control. The transformed yeast cells were selected on synthetically defined (SD), solid medium lacking Leu and Trp (SD/−2). To assess protein–protein interactions, the transformed yeast cells were plated on SD medium lacking Leu, Trp, His, and Ade (SD/−4). Plates were incubated at 30 °C, and the growth of yeast cells was examined after 3 d.

3. Results

3.1. ABA Suppresses Hypocotyl Elongation in Both Light-Grown and Dark-Grown Seedlings in a Dose-Dependent Manner

ABA regulates many aspects of plant growth and development, including inhibition of hypocotyl elongation and root elongation [21,44–47]. Here, we examined the effect of ABA on hypocotyl elongation as well as root elongation in tomato seedlings by time-course analysis. Tomato seedlings were grown in normal light conditions (25 °C light for 16 h and 18 °C dark for 8 h) for seven days (Figure 1a). We found that ABA inhibited hypocotyl elongation at both 0.01 μM and 0.1 μM. 0.1 μM ABA treatment had a stronger inhibitory effect compared to 0.01 μM (Figure 1c). It exhibited a similar effect of ABA-induced suppression on the root elongation (Figure 1d). Next, we checked the effect of ABA on hypocotyl elongation as well as root elongation in dark-grown tomato seedlings (Figure 1b). The results showed that ABA inhibited hypocotyl and root elongation of dark-grown seedlings at both 0.01 μM and 0.1 μM. Compared with that of light-grown seedlings, the differences of inhibition between 0.01 μM and 0.1 μM ABA treatment in the dark-grown seedlings were smaller (Figure 1e), indicating 0.01 μM ABA is sufficient to inhibit

hypocotyl elongation of dark-grown seedlings. Compared with light-grown seedlings, the dark-grown seedlings were more sensitive to ABA (Figure 1c,e). By comparing the hypocotyl length of ABA-treated tomato seedlings grown in light with those grown in dark, we found that light signal was an important factor affecting hypocotyl elongation. Under dark conditions, the hypocotyls of tomato seedlings with or without ABA treatment were significantly longer than that under light conditions (Figure 1c,e). This demonstrates that dark-induced growth of hypocotyls exceeded the inhibition of hypocotyls by ABA.

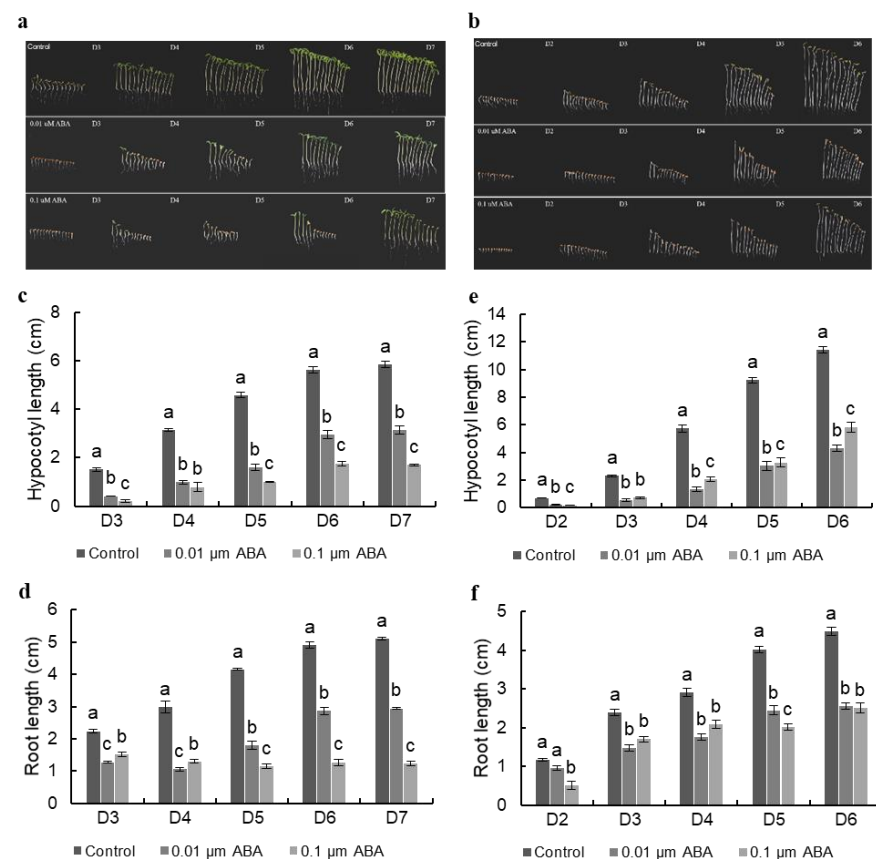


Figure 1. ABA inhibits hypocotyl and root elongation in both light-grown and dark-grown tomato seedlings. (a) Time course of photos of light-grown tomato seedlings on medium containing 0 μM (Control), 0.01 μM, or 0.1 μM ABA. (b) Time course of photos of dark-grown tomato seedlings on medium containing 0 μM (Control), 0.01 μM, or 0.1 μM ABA. (c) Time course of hypocotyl elongation of light-grown tomato seedlings on medium containing 0 μM (Control), 0.01 μM, or 0.1 μM ABA. (d) Time course of root elongation of light-grown tomato seedlings on medium containing 0 μM (Control), 0.01 μM, or 0.1 μM ABA. (e) Time course of hypocotyl elongation of dark-grown tomato seedlings on medium containing 0 μM (Control), 0.01 μM, or 0.1 μM ABA. (f) Time course of root elongation of dark-grown tomato seedlings on medium containing 0 μM (Control), 0.01 μM, or 0.1 μM ABA. For (c–f), each value represents the mean of 15 seedlings with the SE. The experiments were repeated on three occasions with similar results. Different letters indicate significant differences between treatments according to the Fisher’s least significant difference (LSD) test ($p < 0.05$).

3.2. Characterization of D-Clade PP2C (SIPP2C.D) Proteins in Tomato

A previous study reported that ABA inhibits hypocotyl elongation through dephosphorylating H^+ -ATPase [21]. Biochemical analysis revealed that H^+ -ATPases activity is negatively regulated by type 2C protein phosphatase (PP2C) [48]. Further analysis demonstrated that Arabidopsis AtPP2C-D1 of D-Clade PP2Cs inhibited PM H^+ -ATPase activity [33]. AtPP2C-D1 overexpression diminished hypocotyl length, while *pp2c-d1pp2c-d2* double mutants displayed increased hypocotyl [33]. It is interesting to know whether D-Clade PP2C proteins could participate in ABA-mediated inhibition of hypocotyl elongation

in tomato. Firstly, we characterized tomato *SIPP2C.D* proteins. There are 14 *SIPP2C.Ds* in tomato [40]. One conserved PP2C domain existed in 13 out of these 14 *SIPP2C.Ds*, while three PP2C domains existed in Solyc10g078800 (Table 1).

Table 1. Protein length and PP2C domain of *SIPP2C.D* proteins.

Query	PL ¹ (aa ²)	From	To	E-Value	Accession	Short Name
Solyc01g107300	376	42	337	4.67×10^{-62}	cd00143	PP2Cc ³
Solyc01g111730	388	49	356	2.06×10^{-64}	cd00143	PP2Cc
Solyc02g083420	390	48	355	3.33×10^{-64}	cd00143	PP2Cc
Solyc02g092750	366	32	336	4.59×10^{-58}	cd00143	PP2Cc
Solyc03g033340	397	48	355	9.29×10^{-64}	cd00143	PP2Cc
Solyc05g055980	384	53	360	2.43×10^{-68}	cd00143	PP2Cc
Solyc06g065920	374	51	351	2.28×10^{-55}	cd00143	PP2Cc
Solyc09g007080	378	43	350	1.25×10^{-72}	cd00143	PP2Cc
Solyc10g049630	380	34	335	1.20×10^{-59}	cd00143	PP2Cc
Solyc10g055650	339	1	306	1.44×10^{-64}	cd00143	PP2Cc
Solyc10g078800	1312	51	342	3.46×10^{-55}	cd00143	PP2Cc
Solyc10g078800		551	844	1.28×10^{-45}	cd00143	PP2Cc
Solyc10g078800		974	1266	1.36×10^{-54}	cd00143	PP2Cc
Solyc10g078810	438	63	339	2.40×10^{-53}	cd00143	PP2Cc
Solyc10g078820	460	63	341	1.23×10^{-57}	cd00143	PP2Cc
Solyc10g084410	376	42	349	1.38×10^{-72}	cd00143	PP2Cc

¹ PL, protein length. ² aa, amino acid. ³ PP2Cc, serine/threonine phosphatases, family 2C, catalytic domain.

3.3. Expression of *SIPP2C.D* Genes in Response to ABA

To understand the function and transcriptional regulation of *SIPP2C.D* genes on ABA, and to find out whether *SIPP2C.D* genes could potentially participate in ABA signaling pathways and ABA-mediated inhibition of hypocotyl elongation, we first checked the expression patterns of *SIPP2C.Ds* in response to ABA treatment. The results showed that the expression of seven *SIPP2C.D* members were significantly induced by ABA, including Solyc01g111730, Solyc02g083420, Solyc02g083420, Solyc06g065920, Solyc09g007080, Solyc10g049630, and Solyc10g055650. In contrast, Solyc10g084410 was expressed at low levels and downregulated by ABA. No significant difference was observed for Solyc01g107300 and Solyc02g092750. Solyc05g055980 was undetectable both in mock-treated and ABA-treated seedlings (Figure 2). These results indicated that about half of *SIPP2C.Ds* could be responsive to and induced by ABA and might play a role in ABA signaling.

3.4. Organ-Specific Expression of *SIPP2C.D* Genes

To investigate the roles of the *SIPP2C.D* genes in tomato growth and development, the expression patterns of *SIPP2C.Ds* were examined in 11 tomato organs (Figure 3). Four *SIPP2C.Ds*, namely Solyc10g084410, Solyc10g078820, Solyc10g078800, and Solyc10g078810, were absent in all examined organs. Five *SIPP2C.Ds*, namely Solyc05g055980, Solyc06g065920, Solyc10g049630, Solyc01g107300, and Solyc02g092750, were expressed only in certain tissues, while another five *SIPP2C.Ds*, namely Solyc01g111730, Solyc09g007080, Solyc03g033340, Solyc02g083420, and Solyc10g055650, were ubiquitously expressed. Except in young and mature leaves, Solyc09g007080 was expressed highly in the other nine tomato organs. Interestingly, Solyc09g007080 showed relatively higher expression in hypocotyl than in other tested organs. Meanwhile, among the 14 *SIPP2C.D* genes, Solyc09g007080 was the most highly expressed one in hypocotyl. Therefore, Solyc09g007080 was presumably the candidate gene for regulating hypocotyl elongation. The polygenetic tree showed that fourteen tomato *SIPP2C.D* proteins and nine Arabidopsis AtPP2C.D proteins are classified into six groups (Figure 4). Among the 14 tomato *SIPP2C.D* proteins, Solyc09g007080 and Solyc10g084410 were most closely clustered together with AtPP2C.D1 (Figure 4). Although Solyc10g084410 was also classified as a Clade with AtPP2C.D1, it was not expressed in any tissues (Figure 3). Therefore, Solyc09g007080 was named as *SIPP2C.D1* in this study.

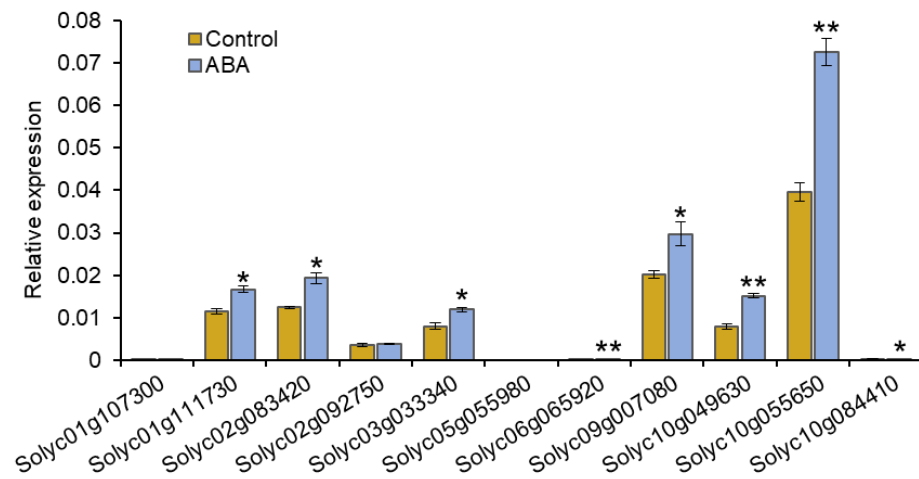


Figure 2. ABA-induced expression patterns of *SIPP2C.D* genes in tomato seedlings. Four-day-old tomato seedlings grown on half-strength Murashige and Skoog (MS) agar medium in dark were subsequently treated with 0.01 μ M ABA for three hours. Total RNA was used for qRT-PCR. The tomato *ACTIN2* gene was used as an internal standard. Values are means \pm SD of three biological replicates. Asterisks refer to data significantly different from 0 μ M ABA (Control); Student's *t*-test: * $p < 0.05$, ** $p < 0.01$.

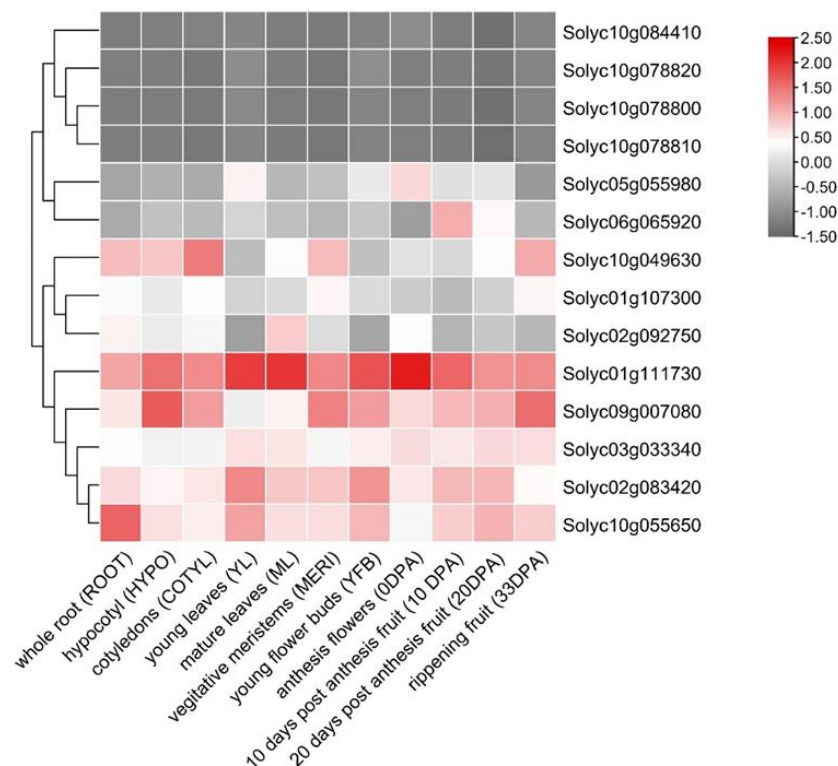


Figure 3. Expression profiles of tomato *SIPP2C.D* genes in various organs. Organ-specific expression of *SIPP2C.D* genes in tomato by using public RNA-sequencing data (The Tomato Genome Consortium, 2012). The values were log₂ transformed with TBtools, and the cluster dendrogram conducted by rows is shown on the left of the heat map. Blocks with grey colors indicate decreased and red ones indicate increased transcription levels. Root, whole root; Hypo, hypocotyl; Cotyl, cotyledon; YL, young leaf; ML, mature leaf; MER, vegetative meristem; YFB, young flower bud; 0 DPA, flower at anthesis; 10 DPA, fruit at 10 DPA; 20 DPA, fruit at 20 DPA; 33 DPA, fruit at 33 DPA.

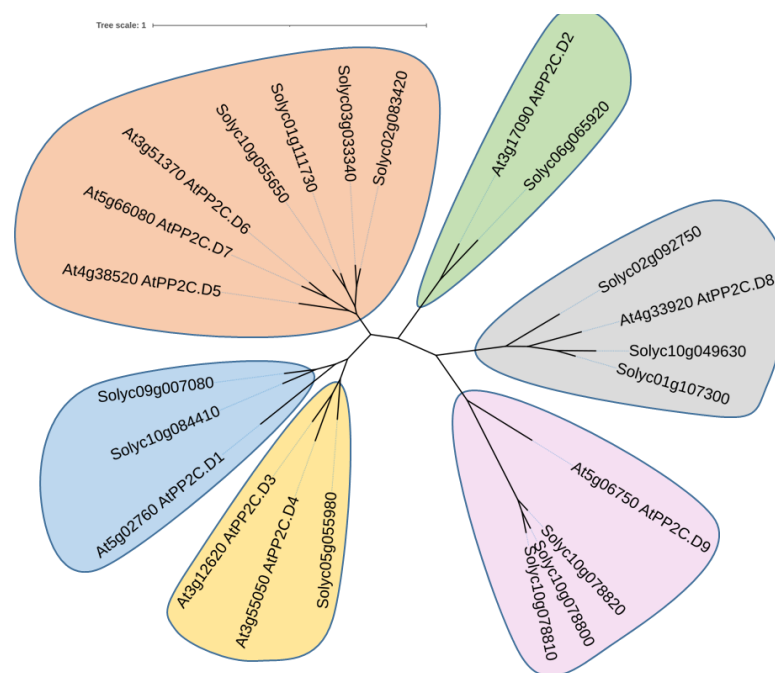


Figure 4. Phylogenetic relationship of PP2C.D proteins from tomato and Arabidopsis. The amino acid sequences of tomato and Arabidopsis PP2C.D proteins were aligned, and a phylogenetic tree was drawn using the maximum-likelihood method with 1000 bootstrap repeats, and the phylogenetic tree was constructed using MEGA X program.

3.5. Expression of *SIPP2C.D1* Gene in Light-Grown and Dark-Grown Seedlings

Hypocotyl elongation is coordinated by light and phytohormones, and *SIPP2C.D1* was found to be strongly expressed in hypocotyl (Figure 3). It is reasonable to speculate that *SIPP2C.D1* might be responsive to the light signal. To figure out the expression pattern of *SIPP2C.D1* gene in response to light, we first tested its expression levels in hypocotyls of dark-grown seedlings when exposed to light. As shown in Figure 5a, *SIPP2C.D1* was increased significantly at 1 h and 6 h of light exposure. In addition, when light-grown tomato seedlings were moved to the dark for 1 h and 6 h, the expression of *SIPP2C.D1* in dissected hypocotyls was significantly downregulated (Figure 5b). The results indicated that expression of *SIPP2C.D1* was strongly upregulated by light.

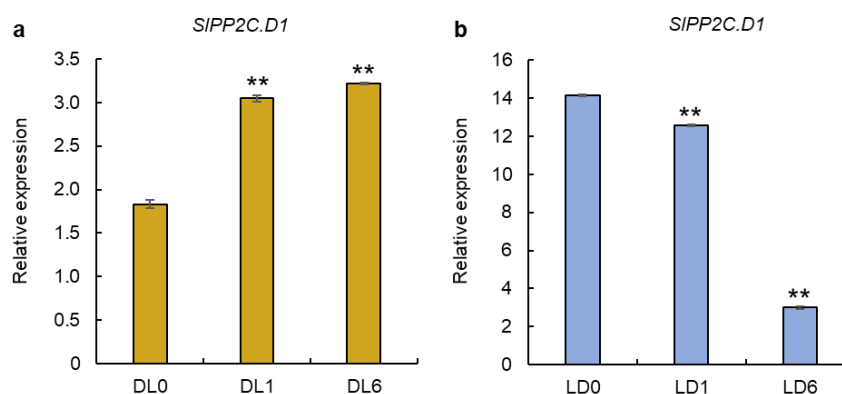


Figure 5. Light-responsive expression patterns of *SIPP2C.D1* in hypocotyls of tomato seedlings. (a) Seven-day-old, dark-grown seedlings were exposed to white light for 0 h (DL0), 1 h (DL1), or 6 h (DL6). (b) Seven-day-old, light-grown seedlings were exposed to darkness for 0 h (LD0), 1 h (LD1), or 6 h (LD6). For (a,b), hypocotyls were dissected for RNA analysis by RT-qPCR. The tomato *ACTIN2* gene was used as an internal standard. Values are means \pm SD of three biological replicates. Asterisks refer to data significantly different from DL0 or LD0; Student's *t*-test: ** $p < 0.01$.

3.6. Characterization of the Interaction between SIPP2C.Ds and SISAUR Proteins

Acid-growth theory mechanism proposed that SAURs inhibit PP2C.D phosphatases to activate PM H⁺-ATPases and promote cell expansion [33]. However, the relationship between tomato *SIPP2C.D1* and SISAUR proteins remains unclear. This prompted us to detect the interaction between *SIPP2C.D1* and SISAURs. The full-length *SIPP2C.D1* protein was fused with the GAL4 DNA binding domain (BD) as “bait”. Full-length SISAUR proteins (Table S2) were expressed as “prey” fusions with the GAL4 activation domain (AD). AD was included as control. The Y2H data showed that, except for three SISAUR proteins (SISAUR3, SISAUR39, and SISAUR90), *SIPP2C.D1*s were found to interact with all the remaining SISAUR proteins (i.e., SISAUR2, SISAUR35, SISAUR40, SISAUR55, SISAUR57, SISAUR59, SISAUR65, and SISAUR70) (Figure 6).

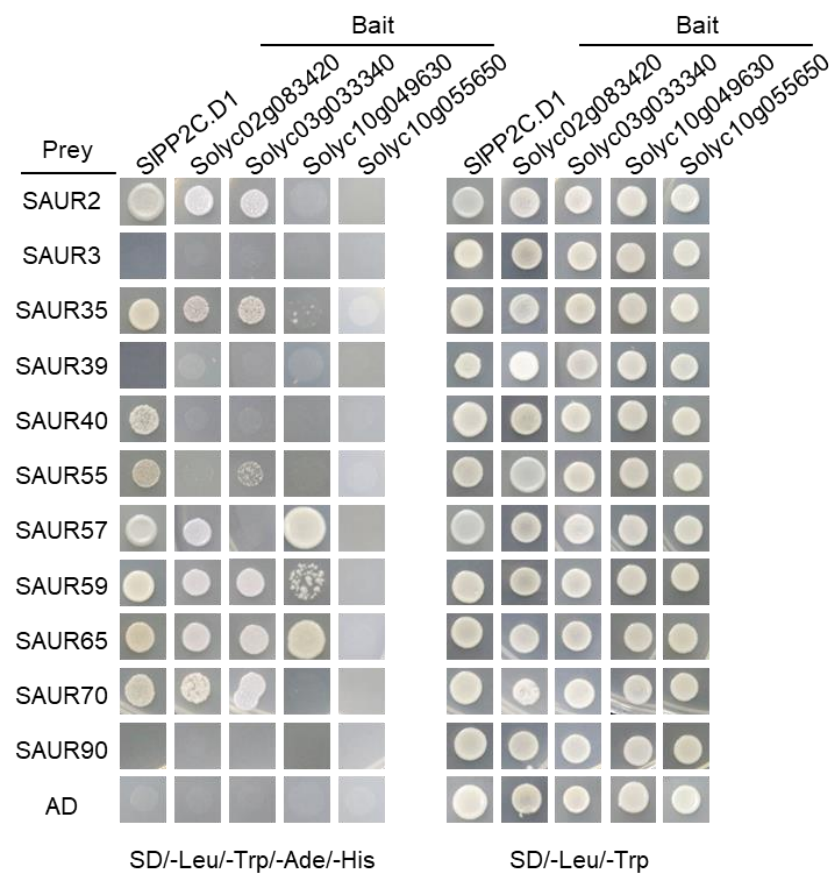


Figure 6. Interaction between SIPP2C.D with SISAUR proteins in the Y2H assay. Tomato SIPP2C.D proteins were fused with the DNA-binding domain (BD) in *pGBKT7*, and full-length SISAUR proteins were fused with the activation domain (AD) in *pGADT7*, respectively. Transformed yeast was grown on synthetic dropout lacking Leu and Trp (SD/−2) as transformation control or selective medium lacking Ade, His, Leu, and Trp (SD/−4) to test protein interactions. The empty *pGADT7* vector was co-transformed with SIPP2C.D proteins in parallel as negative controls.

Additionally, the interaction between other SIPP2C.Ds and SISAURs were also investigated. The results showed that SISAUR2, SISAUR35, SISAUR59, SISAUR65, and SISAUR70 interacted with Solyc02g083420 and Solyc03g033340. In addition, Solyc02g083420 also interacted with SISAUR57, while Solyc03g033340 was also associated with SISAUR55. However, SISAUR3, SISAUR39, and SISAUR90 did not interact with any SIPP2C.D proteins. Solyc10g049630 only interacted with three SISAUR members: SISAUR57, SISAUR59, and SISAUR65. For Solyc10g055650, no interaction was detected with any SISAUR members (Figure 6).

4. Discussion

Although some studies proposed the plant hormone ABA as a plant growth and development stimulator, ABA is generally and substantially considered as a plant growth inhibitor. However, effects of outputs of plant hormones such as ABA on plant growth and development are closely related to the concentration [49]. Basal and low ABA was thought to be required to promote plant growth and development because ABA-deficient mutants exhibited retarded growth and dwarfism, which could be reversed by exogenous ABA treatment [49]. However, ABA was regarded as a general growth inhibitor due to a tight link between stress-inducible growth dwarfism and ABA accumulation. In fact, exogenously applied ABA at high concentrations can mimic stressed conditions, which lead to growth inhibition [49–51]. In consistent with the above notion, our results in this study showed that exogenous ABA both at 0.01 μM and 0.1 μM concentrations significantly inhibited the root and hypocotyl elongation of WT (cv. Ailsa Craig) tomato seedlings (Figure 1). Except for the hormone concentrations, the degree of sensitivity to hormones also depends on the plant varieties. For instance, in tomato seedlings of WT (cv. Rheinlands Ruhm), both 0.1 μM and 1 μM ABA did not have any inhibitory effect on the hypocotyl elongation; the inhibition was only observed until the concentration of ABA reaching 5 μM [45].

Cellular basis of hypocotyl growth is mainly dependent on cell expansion and cell elongation in *Arabidopsis thaliana* [1]. PM H^+ -ATPase has long been considered as a driver of cell growth. PM H^+ -ATPase is an ion pump that exports cellular protons outside the cell. On the one hand, extracellular H^+ activates wall-modification-related proteins, including expansins [5], xyloglucan endotransglycosylase/hydrolases [6], and pectin methylesterases [7], to loosen the cell wall and facilitate cell expansion. On the other hand, electrochemical gradient of protons in turn energizes channel proteins and carriers for nutrient and solute uptake, thereby maintaining the turgor pressure for cell expansion [52]. Upon hypocotyl elongation, PM H^+ -ATPase sits at the nexus of multiple signals, such as auxin [3], ABA [21,53], brassinosteroids [54], peptide [17,26,27], blue light [14], and fusicocin [19]. Notably, the activity of PM H^+ -ATPase is regulated at posttranslational level by phosphorylation and de-phosphorylation. To maintain the phosphorylation status and activity of PM H^+ -ATPase, auxin induced SAUR proteins to interact with and inhibit PP2C.D1, which de-phosphorylates the penultimate threonine residue of PM H^+ -ATPase [33]. There are 14 PP2C.D proteins in tomato (Table 1). Combined with tissue-specific expression pattern (Figure 3) and polygenetic tree (Figure 4), our data suggested that *SIPP2C.D1* (Solyc09g007080) might be involved in hypocotyl growth. Its homologue *AtPP2C.D1* was found to be specifically expressed in the inner part of the apical hook and inhibited PM H^+ -ATPase activity, facilitating apical hook formation [43,55]. Overexpressing *AtPP2C.D1* also led to the reduction in hypocotyl length [33]. Furthermore, the expression of *SIPP2C.D1* was upregulated upon ABA treatment (Figure 2), indicating *SIPP2C.D1* might participate in ABA signaling. However, whether ABA controls PM H^+ -ATPase activity via *SIPP2C.D1* is unknown. In addition, the specific expression region of *SIPP2C.D1* in hypocotyls and its biological function need to be further verified.

In *Arabidopsis*, the main interactants of *AtPP2C.D1* have been demonstrated to be SAUR proteins, including SAUR9, SAUR14, SAUR17, SAUR19, SAUR32, SAUR40, SAUR50, SAUR65, and SAUR72 [33,56,57]. Wang et al. (2020) found PP2C.Ds and SAUR proteins were mutually dominant partners for binding each other [57]. This led us to explore which SAUR proteins interact with *SIPP2C.D1* in tomato. Y2H data showed that *SIPP2C.D1* interacted with all examined SAUR proteins except for SAUR3, SAUR39, and SAUR90 (Figure 6), indicating *SIPP2C.D1* activity may be regulated by these SAUR members and may also act downstream of some signals to modulate the phosphorylation status and activities of specific substrates to regulate plant cell growth. Furthermore, combinations of other four *SIPP2C.D* members and SAUR proteins were characterized at the same time (Figure 6), indicating SAUR-PP2C.D modules ubiquitously exist among different species. Previous findings reminded us that different SAUR proteins have different regulatory

effects on the same PP2C.D, and the same SAUR protein has different ways of acting on different PP2C.D proteins. For example, both AtSAUR17 and AtSAUR50 interacted with AtPP2C.D1; AtSAUR50 inhibited AtPP2C-D1 activity, but AtSAUR17 did not [57]. Additionally, AtSAUR19 could inhibit AtPP2C-D1 activity but not AtPP2C.D2 or AtPP2C.D4 activity [33]. In our study, we found that *SIPP2C.D1* interacted with a subset of SISAUR proteins (Figure 6), and some of these SISAUR proteins can also interact with another four SIPP2C.Ds (Figure 6). However, the different *SIPP2C.D1*/SISAUR interaction modules may contribute to regulating SIPP2C-D1 activity to a different extent, and further studies to clarify their synergistic or inhibitory effects are obviously required.

Lastly, ABA-mediated growth repression may be achieved through an SAUR-PP2C.D functional module. Firstly, SAUR-PP2C.D interaction modules were well-demonstrated to regulate H⁺-ATPases activity, and ABA decreased the phosphorylation level of the penultimate threonine of H⁺-ATPase. Secondly, some *SIPP2C.D* genes were upregulated by ABA treatment, revealing that these SIPP2C.Ds may be ABA-inducible genes. Thirdly, ABA-regulated SAUR expressions were closely associated with ABA-mediated growth repression. ABA could downregulate some growth-promoting SAUR genes such as *AtSAUR19* and *AtSAUR63* [33,58,59]. It is well-known that *AtSAUR19* positively regulates cell expansion by inhibiting PP2C.D phosphatases and then activating PM H⁺-ATPases [33]. Furthermore, previous studies reported that *AtSAUR32* was induced by ABA to regulate ABA-mediated responses under drought stress in Arabidopsis [60,61]. ABA also induced the expressions of SAUR41 subfamily genes to modulate cell expansion, ion homeostasis, and salt tolerance [62]. Our current study demonstrated that both SISAUR59, a homologue to *AtSAUR40* in the Clade A1, and SISAUR65, a homologue to *AtSAUR40* in the Clade C1, interacted with *SIPP2C.D1* and the other three SIPP2C.D members (Figure 6). Again, further investigation on the formation and function of specific SIPP2C.D-SISAUR interaction complexes/modules in response to ABA signaling under different conditions in tomato plants is required.

In conclusion, we found that ABA inhibited hypocotyl and root elongation of light-grown and dark-grown tomato seedlings in a concentration-dependent manner. ABA induced the expression of seven *SIPP2C.D* genes, among which *SIPP2C.D1* was highly expressed in hypocotyl of dark-grown seedlings, and its gene expression was upregulated by ABA and light. Furthermore, we found that different SAUR/PP2C.D interaction modules exist widely in different species, including tomato. The interaction modules of SISAUR and SIPP2C.D were identified by Y2H experiments, which showed *SIPP2C.D1* interacted strongly with SISAUR2, 35, 40, 55, 57, 59, 65, and 70. Solyc02g083420 and Solyc03g033340 both interacted with SISAUR2, 35, 59, 65, and 70. Additionally, Solyc02g083420 interacted with SISAUR57, while Solyc03g033340 was associated with SISAUR55. Solyc10g049630 only interacted with three SISAUR members: SISAUR57, 59, and 65. However, Solyc10g055650 did not interact with any SISAUR members, and SISAUR3, 39, and 90 did not interact with any SIPP2C.D proteins. Altogether, results from this study suggest that further investigation of the regulatory role of ABA in tomato hypocotyls could be focused on the formation and function of SISAUR-SIPP2C.D interaction modules.

Supplementary Materials: The following supporting information can be downloaded at: <https://www.mdpi.com/article/10.3390/agronomy12102542/s1>, Table S1: Primers used in this study. Table S2: The accession numbers of SAUR proteins in this study from SGN database.

Author Contributions: Y.L. designed the experiment; X.Z., S.F. and S.W. conducted the experiment; X.Z. and S.W. analyzed the data; Y.L. wrote the manuscript; Z.Z. and Y.H. revised the manuscript. All authors have read and agreed to the published version of the manuscript.

Funding: This work was financially supported by the National Key Research and Development Program of China (2018YFD1000800), the Natural Science Foundation of Zhejiang Province (LZ20C150001), and the National Natural Science Foundation of China (32102402).

Data Availability Statement: All data used in the study were presented in the submitted article.

Acknowledgments: We wish to thank Zhi-hui Chen from College of Life Sciences, University of Dundee, UK, to his contribution to revise the manuscript.

Conflicts of Interest: The authors declare no conflict of interest.

References

1. Gendreau, E.; Traas, J.; Desnos, T.; Grandjean, O.; Caboche, M.; Hofte, H. Cellular basis of hypocotyl growth in *Arabidopsis thaliana*. *Plant Physiol.* **1997**, *114*, 295–305. [[CrossRef](#)] [[PubMed](#)]
2. Stamm, P.; Kumar, P.P. The phytohormone signal network regulating elongation growth during shade avoidance. *J. Exp. Bot.* **2010**, *61*, 2889–2903. [[CrossRef](#)] [[PubMed](#)]
3. Rayle, D.L.; Cleland, R.E. The Acid Growth Theory of auxin-induced cell elongation is alive and well. *Plant Physiol.* **1992**, *99*, 1271–1274. [[CrossRef](#)] [[PubMed](#)]
4. Rayle, D.L.; Cleland, R. Enhancement of wall loosening and elongation by Acid solutions. *Plant Physiol.* **1970**, *46*, 250–253. [[CrossRef](#)] [[PubMed](#)]
5. McQueen-Mason, S.; Durachko, D.M.; Cosgrove, D.J. Two endogenous proteins that induce cell wall extension in plants. *Plant Cell* **1992**, *4*, 1425–1433. [[PubMed](#)]
6. Nishitani, K.; Vissenberg, K. Roles of the XTH Protein Family in the Expanding Cell. In *The Expanding Cell Plant Cell Monographs*; Verbelen, J.P., Vissenberg, K., Eds.; Springer: Berlin/Heidelberg, Germany, 2006; Volume 6, pp. 89–116.
7. Hocq, L.; Pelloux, J.; Lefebvre, V. Connecting Homogalacturonan-Type Pectin Remodeling to Acid Growth. *Trends Plant Sci.* **2017**, *22*, 20–29. [[CrossRef](#)] [[PubMed](#)]
8. Hager, A. Role of the plasma membrane H⁺-ATPase in auxin-induced elongation growth: Historical and new aspects. *J. Plant Res.* **2003**, *116*, 483–505. [[CrossRef](#)]
9. Katou, K.; Okamoto, H. Symplast as a Functional Unit in Plant Growth. In *International Review of Cytology*; Jeon, K.W., Friedlander, M., Eds.; Academic Press: Cambridge, MA, USA, 1992; Volume 142, pp. 263–304.
10. Takahashi, K.; Hayashi, K.; Kinoshita, T. Auxin activates the plasma membrane H⁺-ATPase by phosphorylation during hypocotyl elongation in *Arabidopsis*. *Plant Physiol.* **2012**, *159*, 632–641. [[CrossRef](#)]
11. Fuglsang, A.T.; Visconti, S.; Drumm, K.; Jahn, T.; Stensballe, A.; Mattei, B.; Jensen, O.N.; Aducci, P.; Palmgren, M.G. Binding of 14-3-3 protein to the plasma membrane H⁺-ATPase AHA2 involves the three C-terminal residues Tyr(946)-Thr-Val and requires phosphorylation of Thr(947). *J. Biol. Chem.* **1999**, *274*, 36774–36780. [[CrossRef](#)]
12. Svennelid, F.; Olsson, A.; Piotrowski, M.; Rosenquist, M.; Ottman, C.; Larsson, C.; Oecking, C.; Sommarin, M. Phosphorylation of Thr-948 at the C terminus of the plasma membrane H⁺-ATPase creates a binding site for the regulatory 14-3-3 protein. *Plant Cell* **1999**, *11*, 2379–2391.
13. Falhof, J.; Pedersen, J.T.; Fuglsang, A.T.; Palmgren, M. Plasma Membrane H⁺-ATPase Regulation in the Center of Plant Physiology. *Mol. Plant* **2016**, *9*, 323–337. [[CrossRef](#)] [[PubMed](#)]
14. Kinoshita, T.; Shimazaki, K. Blue light activates the plasma membrane H⁺-ATPase by phosphorylation of the C-terminus in stomatal guard cells. *EMBO J.* **1999**, *18*, 5548–5558. [[CrossRef](#)] [[PubMed](#)]
15. Okumura, M.; Takahashi, K.; Inoue, S.; Kinoshita, T. Evolutionary appearance of the plasma membrane H⁺-ATPase containing a penultimate threonine in the bryophyte. *Plant Signal. Behav.* **2012**, *7*, 979–982. [[CrossRef](#)]
16. Okumura, M.; Inoue, S.; Takahashi, K.; Ishizaki, K.; Kohchi, T.; Kinoshita, T. Characterization of the plasma membrane H⁺-ATPase in the liverwort *Marchantia polymorpha*. *Plant Physiol.* **2012**, *159*, 826–834. [[CrossRef](#)] [[PubMed](#)]
17. Nuhse, T.S.; Bottrill, A.R.; Jones, A.M.; Peck, S.C. Quantitative phosphoproteomic analysis of plasma membrane proteins reveals regulatory mechanisms of plant innate immune responses. *Plant J.* **2007**, *51*, 931–940. [[CrossRef](#)]
18. Cleland, R.E. Fusicoccin-induced growth and hydrogen ion excretion of *Avena* coleoptiles: Relation to auxin responses. *Planta* **1976**, *128*, 201–206. [[CrossRef](#)]
19. Marre, E. Fusicoccin: A Tool in Plant Physiology. *Annu. Rev. Plant Physiol.* **1979**, *30*, 273–288. [[CrossRef](#)]
20. Chen, Y.; Hoehenwarter, W.; Weckwerth, W. Comparative analysis of phytohormone-responsive phosphoproteins in *Arabidopsis thaliana* using TiO₂-phosphopeptide enrichment and mass accuracy precursor alignment. *Plant J.* **2010**, *63*, 1–17. [[CrossRef](#)]
21. Hayashi, Y.; Takahashi, K.; Inoue, S.; Kinoshita, T. Abscisic acid suppresses hypocotyl elongation by dephosphorylating plasma membrane H⁺-ATPase in *Arabidopsis thaliana*. *Plant Cell Physiol.* **2014**, *55*, 845–853. [[CrossRef](#)]
22. Duby, G.; Poreba, W.; Piotrowiak, D.; Bobik, K.; Derua, R.; Waelkens, E.; Boutry, M. Activation of plant plasma membrane H⁺-ATPase by 14-3-3 proteins is negatively controlled by two phosphorylation sites within the H⁺-ATPase C-terminal region. *J. Biol. Chem.* **2009**, *284*, 4213–4221. [[CrossRef](#)]
23. Fuglsang, A.T.; Guo, Y.; Cuin, T.A.; Qiu, Q.; Song, C.; Kristiansen, K.A.; Bych, K.; Schulz, A.; Shabala, S.; Schumaker, K.S.; et al. *Arabidopsis* protein kinase PKS5 inhibits the plasma membrane H⁺-ATPase by preventing interaction with 14-3-3 protein. *Plant Cell* **2007**, *19*, 1617–1634. [[CrossRef](#)] [[PubMed](#)]
24. Fuglsang, A.T.; Borch, J.; Bych, K.; Jahn, T.P.; Roepstorff, P.; Palmgren, M.G. The binding site for regulatory 14-3-3 protein in plant plasma membrane H⁺-ATPase: Involvement of a region promoting phosphorylation-independent interaction in addition to the phosphorylation-dependent C-terminal end. *J. Biol. Chem.* **2003**, *278*, 42266–42272. [[CrossRef](#)] [[PubMed](#)]

25. Rudashevskaya, E.L.; Ye, J.; Jensen, O.N.; Fuglsang, A.T.; Palmgren, M.G. Phosphosite mapping of P-type plasma membrane H⁺-ATPase in homologous and heterologous environments. *J. Biol. Chem.* **2012**, *287*, 4904–4913. [[CrossRef](#)] [[PubMed](#)]
26. Haruta, M.; Sabat, G.; Stecker, K.; Minkoff, B.B.; Sussman, M.R. A peptide hormone and its receptor protein kinase regulate plant cell expansion. *Science* **2014**, *343*, 408–411. [[CrossRef](#)]
27. Fuglsang, A.T.; Kristensen, A.; Cuin, T.A.; Schulze, W.X.; Persson, J.; Thuesen, K.H.; Ytting, C.K.; Oehlenschlaeger, C.B.; Mahmood, K.; Sondergaard, T.E.; et al. Receptor kinase-mediated control of primary active proton pumping at the plasma membrane. *Plant J.* **2014**, *80*, 951–964. [[CrossRef](#)]
28. Lin, W.; Zhou, X.; Tang, W.; Takahashi, K.; Pan, X.; Dai, J.; Ren, H.; Zhu, X.; Pan, S.; Zheng, H.; et al. TMK-based cell-surface auxin signalling activates cell-wall acidification. *Nature* **2021**, *599*, 278–282. [[CrossRef](#)]
29. Pei, D.; Hua, D.; Deng, J.; Wang, Z.; Song, C.; Wang, Y.; Wang, Y.; Qi, J.; Kollist, H.; Yang, S.; et al. Phosphorylation of the plasma membrane H⁺-ATPase AHA2 by BAK1 is required for ABA-induced stomatal closure in Arabidopsis. *Plant Cell* **2022**, *34*, 2708–2729. [[CrossRef](#)]
30. Kerk, D.; Templeton, G.; Moorhead, G.B. Evolutionary radiation pattern of novel protein phosphatases revealed by analysis of protein data from the completely sequenced genomes of humans, green algae, and higher plants. *Plant Physiol.* **2008**, *146*, 351–367. [[CrossRef](#)]
31. Cohen, P. The structure and regulation of protein phosphatases. *Annu. Rev. Biochem.* **1989**, *58*, 453–508.
32. Cohen, P.T. Novel protein serine/threonine phosphatases: Variety is the spice of life. *Trends Biochem. Sci.* **1997**, *22*, 245–251. [[CrossRef](#)]
33. Spartz, A.K.; Ren, H.; Park, M.Y.; Grandt, K.N.; Lee, S.H.; Murphy, A.S.; Sussman, M.R.; Overvoorde, P.J.; Gray, W.M. SAUR Inhibition of PP2C-D Phosphatases Activates Plasma Membrane H⁺-ATPases to Promote Cell Expansion in Arabidopsis. *Plant Cell* **2014**, *26*, 2129–2142. [[CrossRef](#)] [[PubMed](#)]
34. Ren, H.; Gray, W.M. SAUR Proteins as Effectors of Hormonal and Environmental Signals in Plant Growth. *Mol. Plant* **2015**, *8*, 1153–1164. [[CrossRef](#)]
35. Chen, K.; Li, G.J.; Bressan, R.A.; Song, C.P.; Zhu, J.K.; Zhao, Y. Abscisic acid dynamics, signaling, and functions in plants. *J. Integr. Plant Biol.* **2020**, *62*, 25–54. [[CrossRef](#)] [[PubMed](#)]
36. Brookbank, B.P.; Patel, J.; Gazzarrini, S.; Nambara, E. Role of Basal ABA in Plant Growth and Development. *Genes* **2021**, *12*, 1936. [[CrossRef](#)] [[PubMed](#)]
37. Wakabayashi, K.; Sakurai, N.; Kuraishi, S. Role of the outer tissue in abscisic acid-mediated growth suppression of etiolated squash hypocotyl segments. *Physiol. Plant.* **1989**, *75*, 151–156. [[CrossRef](#)]
38. Miao, R.; Yuan, W.; Wang, Y.; Garcia-Maquilon, I.; Dang, X.L.; Li, Y.; Zhang, J.H.; Zhu, Y.Y.; Rodriguez, P.L.; Xu, W.F. Low ABA concentration promotes root growth and hydrotropism through relief of ABA INSENSITIVE 1-mediated inhibition of plasma membrane H⁺-ATPase 2. *Sci. Adv.* **2021**, *7*, eabd4113. [[CrossRef](#)] [[PubMed](#)]
39. Merlot, S.; Gosti, F.; Guerrier, D.; Vavasseur, A.; Giraudat, J. The ABI1 and ABI2 protein phosphatases 2C act in a negative feedback regulatory loop of the abscisic acid signalling pathway. *Plant J.* **2001**, *25*, 295–303. [[CrossRef](#)]
40. Qiu, J.; Ni, L.; Xia, X.; Chen, S.; Zhang, Y.; Lang, M.; Li, M.; Liu, B.; Pan, Y.; Li, J.; et al. Genome-Wide Analysis of the Protein Phosphatase 2C Genes in Tomato. *Genes* **2022**, *13*, 604. [[CrossRef](#)]
41. Chen, C.; Chen, H.; Zhang, Y.; Thomas, H.R.; Frank, M.H.; He, Y.; Xia, R. TBtools: An Integrative Toolkit Developed for Interactive Analyses of Big Biological Data. *Mol. Plant* **2020**, *13*, 1194–1202. [[CrossRef](#)]
42. Kumar, S.; Stecher, G.; Li, M.; Nkya, C.; Tamura, K. MEGA X: Molecular Evolutionary Genetics Analysis across Computing Platforms. *Mol. Biol. Evol.* **2018**, *35*, 1547–1549. [[CrossRef](#)]
43. Ren, H.; Park, M.Y.; Spartz, A.K.; Wong, J.H.; Gray, W.M. A subset of plasma membrane-localized PP2C.D phosphatases negatively regulate SAUR-mediated cell expansion in Arabidopsis. *PLoS Genet.* **2018**, *14*, e1007455. [[CrossRef](#)] [[PubMed](#)]
44. Lorrain, R.; Boccaccini, A.; Ruta, V.; Possenti, M.; Costantino, P.; Vittorioso, P. Abscisic acid inhibits hypocotyl elongation acting on gibberellins, DELLA proteins and auxin. *AoB Plants* **2018**, *10*, ply061. [[PubMed](#)]
45. Humplik, J.F.; Bergougnoux, V.; Jandova, M.; Simura, J.; Pencik, A.; Tomanec, O.; Rolcik, J.; Novak, O.; Fellner, M. Endogenous abscisic acid promotes hypocotyl growth and affects endoreduplication during dark-induced growth in tomato (*Solanum lycopersicum* L.). *PLoS ONE* **2015**, *10*, e0117793. [[CrossRef](#)] [[PubMed](#)]
46. Zhu, J.D.; Wang, J.; Guo, X.N.; Shang, B.S.; Yan, H.R.; Zhang, X.; Zhao, X. A high concentration of abscisic acid inhibits hypocotyl phototropism in *Gossypium arboreum* by reducing accumulation and asymmetric distribution of auxin. *J. Exp. Bot.* **2021**, *72*, 6365–6381. [[CrossRef](#)] [[PubMed](#)]
47. Li, J.; Hettenhausen, C.; Sun, G.; Zhuang, H.; Li, J.H.; Wu, J. The parasitic plant *Cuscuta australis* is highly insensitive to abscisic acid-induced suppression of hypocotyl elongation and seed germination. *PLoS ONE* **2015**, *10*, e0135197. [[CrossRef](#)]
48. Hayashi, Y.; Nakamura, S.; Takemiya, A.; Takahashi, Y.; Shimazaki, K.; Kinoshita, T. Biochemical characterization of in vitro phosphorylation and dephosphorylation of the plasma membrane H⁺-ATPase. *Plant Cell Physiol.* **2010**, *51*, 1186–1196. [[CrossRef](#)]
49. Humplik, J.F.; Bergougnoux, V.; Van Volkenburgh, E. To Stimulate or Inhibit? That Is the Question for the Function of Abscisic Acid. *Trends Plant Sci.* **2017**, *22*, 830–841. [[CrossRef](#)]
50. Cramer, G.R.; Quarrie, S.A. Abscisic acid is correlated with the leaf growth inhibition of four genotypes of maize differing in their response to salinity. *Funct. Plant Biol.* **2002**, *29*, 111–115. [[CrossRef](#)]

51. Zhang, J.; Davies, W.J. Does ABA in the Xylem Control the Rate of Leaf Growth in Soil-Dried Maize and Sunflower Plants? *J. Exp. Bot.* **1990**, *41*, 1125–1132. [[CrossRef](#)]
52. Sondergaard, T.E.; Schulz, A.; Palmgren, M.G. Energization of transport processes in plants. roles of the plasma membrane H⁺-ATPase. *Plant Physiol.* **2004**, *136*, 2475–2482. [[CrossRef](#)]
53. Hayashi, M.; Inoue, S.; Takahashi, K.; Kinoshita, T. Immunohistochemical detection of blue light-induced phosphorylation of the plasma membrane H⁺-ATPase in stomatal guard cells. *Plant Cell Physiol.* **2011**, *52*, 1238–1248. [[CrossRef](#)] [[PubMed](#)]
54. Witthoft, J.; Caesar, K.; Elgass, K.; Huppenberger, P.; Kilian, J.; Schleifenbaum, F.; Oecking, C.; Harter, K. The activation of the Arabidopsis P-ATPase 1 by the brassinosteroid receptor BRI1 is independent of threonine 948 phosphorylation. *Plant Signal. Behav.* **2011**, *6*, 1063–1066. [[CrossRef](#)] [[PubMed](#)]
55. Du, M.; Bou Daher, F.; Liu, Y.; Steward, A.; Tillmann, M.; Zhang, X.; Wong, J.H.; Ren, H.; Cohen, J.D.; Li, C.; et al. Biphasic control of cell expansion by auxin coordinates etiolated seedling development. *Sci. Adv.* **2022**, *8*, eabj1570. [[CrossRef](#)] [[PubMed](#)]
56. Sun, N.; Wang, J.; Gao, Z.; Dong, J.; He, H.; Terzaghi, W.; Wei, N.; Deng, X.W.; Chen, H. Arabidopsis SAURs are critical for differential light regulation of the development of various organs. *Proc. Natl. Acad. Sci. USA* **2016**, *113*, 6071–6076. [[CrossRef](#)]
57. Wang, J.; Sun, N.; Zhang, F.; Yu, R.; Chen, H.; Deng, X.W.; Wei, N. SAUR17 and SAUR50 Differentially Regulate PP2C-D1 during Apical Hook Development and Cotyledon Opening in Arabidopsis. *Plant Cell* **2020**, *32*, 3792–3811. [[CrossRef](#)]
58. Kodaira, K.S.; Qin, F.; Tran, L.S.; Maruyama, K.; Kidokoro, S.; Fujita, Y.; Shinozaki, K.; Yamaguchi-Shinozaki, K. Arabidopsis Cys2/His2 zinc-finger proteins AZF1 and AZF2 negatively regulate abscisic acid-repressive and auxin-inducible genes under abiotic stress conditions. *Plant Physiol.* **2011**, *157*, 742–756. [[CrossRef](#)]
59. Chae, K.; Isaacs, C.G.; Reeves, P.H.; Maloney, G.S.; Muday, G.K.; Nagpal, P.; Reed, J.W. Arabidopsis SMALL AUXIN UP RNA63 promotes hypocotyl and stamen filament elongation. *Plant J.* **2012**, *71*, 684–697. [[CrossRef](#)]
60. He, Y.; Liu, Y.; Li, M.; Lamin-Samu, A.T.; Yang, D.; Yu, X.; Izhar, M.; Jan, I.; Ali, M.; Lu, G. The Arabidopsis SMALL AUXIN UP RNA32 Protein Regulates ABA-Mediated Responses to Drought Stress. *Front. Plant Sci.* **2021**, *12*, 625493. [[CrossRef](#)]
61. Wu, J.; Liu, S.; He, Y.; Guan, X.; Zhu, X.; Cheng, L.; Wang, J.; Lu, G. Genome-wide analysis of SAUR gene family in Solanaceae species. *Gene* **2012**, *509*, 38–50. [[CrossRef](#)]
62. Qiu, T.; Qi, M.; Ding, X.; Zheng, Y.; Zhou, T.; Chen, Y.; Han, N.; Zhu, M.; Bian, H.; Wang, J. The SAUR41 subfamily of SMALL AUXIN UP RNA genes is abscisic acid inducible to modulate cell expansion and salt tolerance in *Arabidopsis thaliana* seedlings. *Ann. Bot.* **2020**, *125*, 805–819. [[CrossRef](#)]